Report

Drosophila timeless2 Is Required for Chromosome Stability and Circadian Photoreception

Clara Benna,[1] Silvia Bonaccorsi,[2] Corinna Wülbeck,[3]
Charlotte Helfrich-Förster,[3] Maurizio Gatti,[2]
Charalambos P. Kyriacou,[4] Rodolfo Costa,[1,*]
and Federica Sandrelli[1]

[1]Dipartimento di Biologia, Università degli Studi di Padova, via Ugo Bassi 58/B, 35131 Padova, Italy
[2]Dipartimento di Genetica e Biologia Molecolare and Istituto di Biologia e Patologia Molecolare del Consiglio Nazionale delle Ricerche, Università degli Studi di Roma "La Sapienza," 00185 Roma, Italy
[3]Institute of Zoology, University of Regensburg, 93040 Regensburg, Germany
[4]Department of Genetics, University of Leicester, Leicester LE1 7RH, UK

Summary

In Drosophila, there are two timeless paralogs, timeless1 (tim1) and timeless2 (tim2, or timeout) [1, 2]. Phylogenetic analyses suggest that tim1 originated as a duplication of tim2 around the time of the Cambrian explosion [3]. The function of tim1 as a canonical circadian component is well established [4], but the role of tim2 in the fly is poorly understood. Many organisms possess a single tim2-like gene that has been implicated in DNA synthesis and, in the case of mammals, somewhat controversially, in circadian rhythmicity [2, 5]. Here we analyze the structure and the functional role of fly tim2. tim2 is a large locus (∼75 kb) that harbors several transcribed intronic sequences. Using insertional mutations and tissue-specific RNA interference-mediated downregulation, we find that tim2 is an essential gene required for normal DNA metabolism and chromosome integrity. Moreover, tim2 is involved in light entrainment of the adult circadian clock, via its expression in the T1 basket cells of the optic lobes. tim2's residual role in light entrainment thus provides an evolutionary link that may explain why its derived paralog, tim1, came to play such a major role in both circadian photosensitivity and core clock function.

Results and Discussion

tim2 Genomic Structure

The Drosophila melanogaster tim2 locus spans 75 kb and is organized in 18 exons and 17 introns [1, 2]. The second and the eleventh introns harbor two actively transcribed sequences (Figure 1A; see also the Supplemental Results available online). Of these, only the embedded sequence indicated as 2mit in intron 11 might represent a genuine protein-coding "nested" gene, because its putative AUG codon for the longest predicted open reading frame is surrounded by a canonical −3 to +4 translational start sequence (Figures 1A, 1B, and 1F; Supplemental Results) [6].

tim2 Expression during Development

To analyze the overall tim2 expression profile, we amplified a fragment common to all tim2 mRNA isoforms by quantitative PCR (qPCR). We found significant variation in tim2 expression levels during development (Figure 2A; see also Figure S1).

In 12 hr:12 hr light:dark conditions (LD12:12), tim2 mRNA levels in adult fly heads were characterized by a significant oscillating profile, with a peak of expression just after lights-off, between ZT12 and ZT15 (with ZT0 corresponding to lights-on and ZT12 to lights-off; Figure 2B). These data are in agreement with a previous transcriptome report [7]. After 2 days of constant darkness (DD), tim2 mRNA expression in heads became constitutive. In bodies, the tim2 mRNA level was 7-fold higher than in heads (Figure 2B) and was constitutively expressed in LD12:12 (Figure 2C).

In adult brains, tim2 mRNA hybridization signals were observed in the optic lobes, predominantly in the second optic neuropile (medulla), with a pattern resembling a modular array (Figures 3A and 3B). Additional expression was visualized in ellipsoid body fibers of the central complex (Figure 3A), and a weak tim2 signal was identified in mushroom bodies (data not shown). No tim2 mRNA expression was found in circadian clock neurons, as shown by cohybridization experiments with both the tim2 probe and specific probes for circadian clock such as cry (Figures 3D–3F) or tim1 mRNA (data not shown).

To map tim2 mRNA localization in the medulla, we performed cohybridization experiments with tim2 and lacZ mRNA probes on T1Gal4-UASlacZ adult brains. The T1Gal4 driver is mainly expressed in the T1 basket neurons, and at lower levels in mushroom bodies [8]. T1 basket cells have somas located in the medulla cortex and T-shaped projections, one directed toward the external region of the medulla and the other to the lamina (the first optic neuropile); the latter projection arborizes in basket-shape processes that surround each lamina cartridge [9, 10]. The tim2 mRNA signals colocalized with lacZ in the soma of T1 basket cells (Figures 3G–3I). Additional tim2 hybridization signals were observed in the medulla neuronal terminations (Figures 3G–3I), indicating that tim2 is subject to neuronal transport and translational controls. Local control of mRNA translation within dendrites has been demonstrated in both Drosophila and mammals [11], and it is believed to be critical for long-lasting synaptic plasticity [12].

tim2 Is an Essential Gene

In worms and mice, tim2 ortholog knockdown (KD) or knockout results in early embryonic lethality [2, 13]. We characterized five Drosophila PBtim2⁻ mutant alleles generated by independent insertions of a piggyBac (PB) transposon in noncoding regions of tim2 (see Supplemental Experimental Procedures for details). Four out of five PBtim2⁻ mutant alleles (PBtim2^c06976, PBtim2^c01927, PBtim2^f00297, and PBtim2^f05903) were homozygous lethal. Lethality occurred mainly ∼12 hr after puparium formation (APF; Figures S2 and S3). Flies heterozygous for any of these PBtim2⁻ alleles were fully viable. Flies homozygous for the PBtim2^c03963 insertion were also viable and displayed normal tim2 mRNA levels, whereas qPCR performed with third-instar larvae homozygous for the four PBtim2⁻ lethal alleles revealed tim2 mRNA decreases
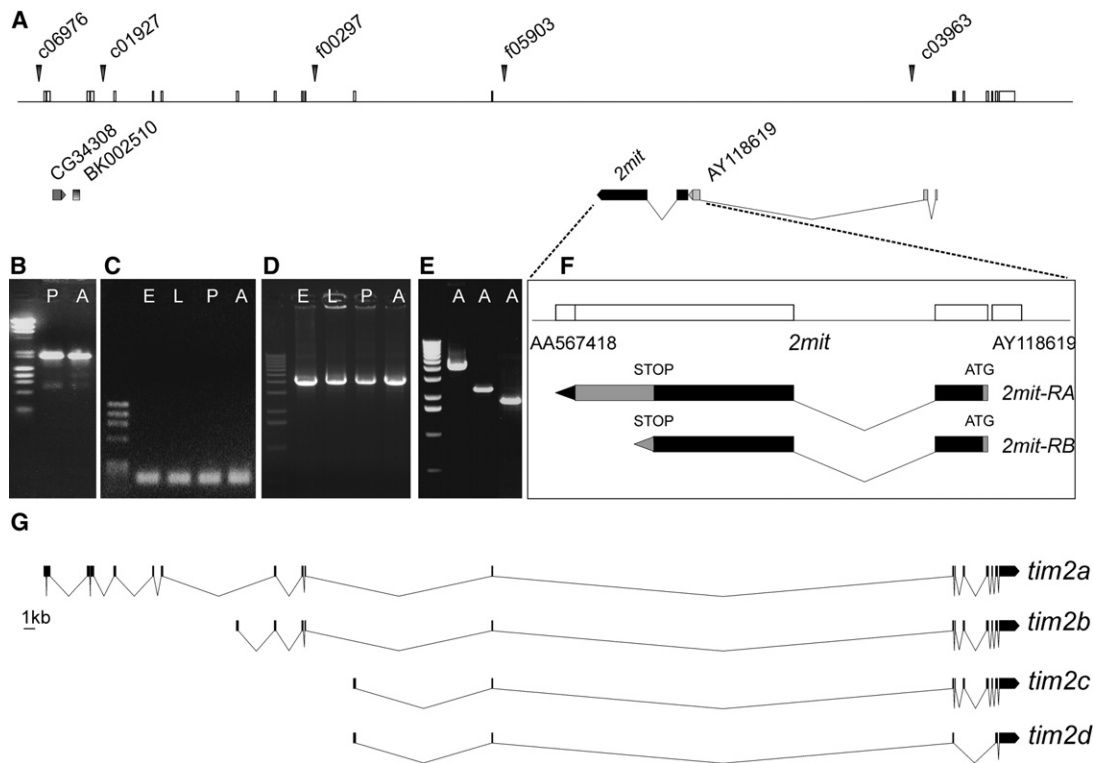
Figure 1. *tim2* Locus Organization and Expression

(A) Schematic representation of *tim2* genomic structure. Arrowheads indicate the position of *piggyBac* (*PB*) element insertions in *PBtim2*⁻ alleles. Below the *tim2* genomic region, positions and splicing sites of *tim2* embedded sequences (*CG34308*, *BK002510*, *2mit*, and *AY118619*) are indicated.

(B–E) Transcription of *tim2* sequences during development. The following abbreviations are used: E, 24 hr embryos; L, third-instar larvae; P, pupae; A, adults. DNA markers were loaded in the left lane of each panel: λ (HindIII) and ΦX174 (HaeI) (B); ΦX174 (HaeI) (C); 1 kb DNA ladder (Invitrogen) (D and E).

(B) *2mit* ~2 kb 3′ untranslated region.

(C) *AY118619* ~130 bp 3′ rapid amplification of cDNA ends.

(D) *tim2* ~4.3 kb mRNA isoform.

(E) *tim2* ~4.3, 2.5, and 1.9 kb mRNA isoforms.

(F) Details of intron 11 indicating the *2mit* and annotated *AY118619* embedded sequences (white boxes) and the *2mit* mRNA isoforms (RA and RB, black boxes). Gray boxes and arrow indicate 5′ and 3′ untranslated regions (UTRs); the black arrow in *2mit*-RA indicates the portion of the 3′UTR that includes *AA567418* EST.

(G) Schematic representation of *tim2* mRNA isoforms. *Drosophila tim2* transcription produces a major ~4.3 kb mRNA throughout development and three additional smaller 5′ alternative spliced transcripts expressed at very low levels (Supplemental Results). From top to bottom: ~4.3 kb *tim2a* mRNA canonical form, ~2.9 kb *tim2b* isoform, ~2.5 kb *tim2c* isoform, ~1.9 kb *tim2d* isoform.

(ranging from 85% to 98%) compared to controls (Table 1; see also Figure S2). For the *PBtim2*[c06976] mutant, *tim2* mRNA levels were also determined in heterozygous larvae, which showed ~36% decrease compared to their wild-type counterparts (Table 1).

We investigated whether the *PB* insertions modify the expression of the internally transcribed sequences of the *tim2* locus. Significant decreases in *CG34308* mRNA levels were detected in larvae homozygous for *PBtim2*[c06976], *PBtim2*[c01927], and *PBtim2*[f00297], whereas *PBtim2*[f05903] homozygotes displayed normal levels of this mRNA (Table 1). *BK002510* transcription was significantly perturbed only in the *PBtim2*[c06976] mutant strain, which showed ~3-fold increase in *BK002510* mRNA levels. *2mit* mRNA levels remained comparable to controls in all *PB* mutants except *PBtim2*[c03963] (Table 1). However, the lethal phenotype is specifically associated with the *tim2* transcription decreases, because *PBtim2*[f05903] mutants exhibit a strong reduction in *tim2* mRNA but normal levels of *GC34308* and *BK002510* mRNAs.

Subsequently, we generated three independent transgenic lines (*tim2* KD[16], *tim2* KD[26b], and *tim2* KD[26i]) carrying a *UAS*-bearing construct for *tim2* KD designed against a region common to all *tim2* mRNA isoforms. To induce an early and general *tim2* silencing, we employed an *Actin5C-Gal4* (*ActGal4*) driver. The use of this driver resulted in different degrees of *tim2* mRNA depletion in third-instar larvae of the different lines, ranging from 59% in KD[26b] to 35% in KD[26i] (Figure S3). The expression of the *tim2* KD construct did not affect the mRNA levels of two predicted off-target genes (Figure S3 legend). *ActGal4*-driven *tim2* KD resulted in lethality in late pupal stages, with head and eyes more affected than either thorax or abdomen (72–96 hr APF; Figures S2 and S3).

tim2 Is Required for Chromosome Integrity

Mammalian TIM (mTIM) associates with the replisome, preventing accumulation of single-stranded DNA at replication forks and facilitating DNA replication [14, 15]. In addition, mTIM interacts with the ATR-ATRIP complex and the CHK1 kinase [16], both involved in the signaling pathway of the S phase and G2/M checkpoints [17]. Consistent with these findings, mTIM downregulation leads to an increase of both chromosome aberrations and sister chromatid exchanges in
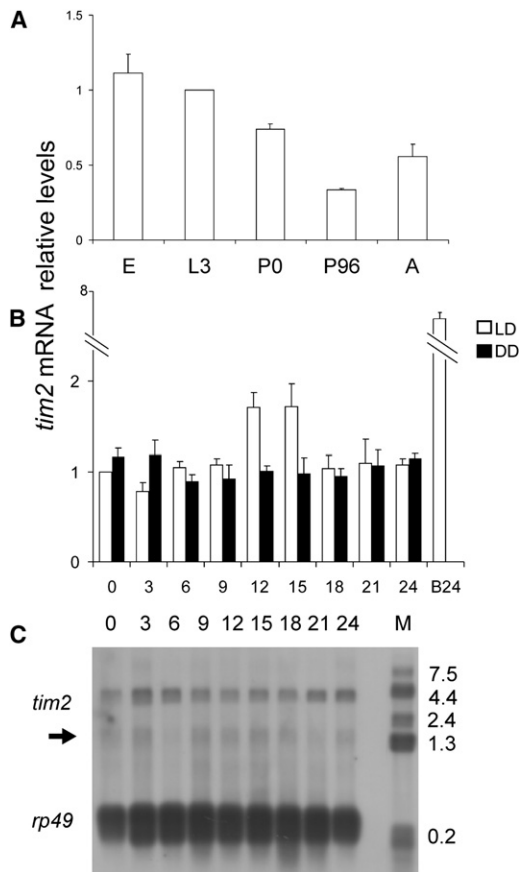
Figure 2. *tim2* Expression in Wild-Type Flies

(A) *tim2* mRNA levels (mean ± standard error of the mean [SEM]) during development and in wild-type (w^{1118}) adult heads. The following abbreviations are used: E, 24 hr embryos; L3, third-instar larvae; P0, early pupae; P96, pupae 96 hr after puparium formation; A, adult heads (plot of four replicates; $F_{4,17} = 44.6$, $p < 0.0001$; Newman-Keuls post hoc test: L3 versus P0, $p < 0.001$; P0 versus P96, $p < 0.0002$; P96 versus A, $p < 0.05$) (see also Figure S1).

(B) *tim2* mRNA levels (mean ± SEM) in adult heads sampled every 3 hr in 12 hr:12 hr light:dark (LD12:12, white bars) and constant darkness (DD, black bars) conditions. B24 indicates *tim2* mRNA levels in bodies at ZT24 (with ZT0 corresponding to lights-on and ZT12 to lights-off). For each condition, four replicates were performed. In 12:12 LD, significant variations in *tim2* mRNA levels were revealed ($F_{8,34} = 6.05$, $p < 0.0001$). Cross-correlation of the ZT means to a sine wave with a 24 hr period was also significant ($r = 0.78$, $p = 0.023$; p values obtained by Monte Carlo simulations). In DD, no significant variations in *tim2* mRNA levels were revealed ($F_{8,25} = 0.77$, $p = 0.63$, not significant).

(C) Northern blot from adult bodies sampled every 3 hr in 12:12 LD. *tim2* indicates the major ~4.3 kb *tim2* transcript. Arrow indicates a nonspecific signal not confirmed by quantitative PCR.

nonmutagenized cells [18]. To address the role of TIM2 in *Drosophila* chromosome stability, we cytologically characterized mitotic chromosomes in *tim2* mutants under both physiological and genotoxic stress conditions. Brains from larvae either homozygous or hemizygous (over a chromosome carrying a deletion that removes the *tim2* locus) for each of the four lethal *PBtim2⁻* mutant alleles consistently exhibited a substantial increase in the number of metaphases with chromosome aberrations compared to controls (Figures 4A–4C and 4L). The frequencies of aberrant metaphases observed in either homozygous or hemizygous larvae were comparable for all of the *PBtim2⁻* mutant alleles characterized except

PBtim2^f05903 (Figure 4L). This strongly suggests that *PBtim2^c06976*, *PBtim2^c01927*, and *PBtim2^f00297* are genetically null mutations whereas *PBtim2^f05903* is a hypomorphic allele.

To assess the existence of a genetic interaction between *tim2* and the *Drosophila ATR* ortholog *mei-41*, we examined *mei-41^29D*; *PBtim2^c06976* double mutants. Larval brains from these double mutants showed a dramatic increase in the frequency of aberrant metaphases with respect to either single mutant (Figures 4D–4G and 4M). The prevalent defect in *mei-41^29D*; *PBtim2^c06976* mutant brains consisted of metaphases with extensive chromosome fragmentation, a phenotype rarely observed in either *mei-41^29D* or any of the *PBtim2⁻* single mutants characterized (Figures 4D–4G). Given that both *mei-41^29D* and *PBtim2^c06976* behave as null mutations (this study; [19]), these results suggest that *tim2* and *mei-41* do not function in a single linear pathway leading to chromosome aberrations.

Deficiency of human TIM2 leads to DNA damage by affecting replisome function [14, 15, 18] and compromises the ATR-mediated checkpoint [16]. The strong synergistic effect of *mei-41* and *tim2* mutations in the production of chromosome damage argues against the possibility that *mei-41* and *tim2* solely function in the signaling cascade of the DNA damage checkpoint. Studies in *Drosophila* have shown that in addition to the DNA damage-dependent G2/M checkpoint, *mei-41* (ATR) is also involved in DNA double-strand break (DSB) repair independently of this checkpoint [20, 21]. These findings suggest a model for the *mei-41-tim2* interaction (Figure 4N). We propose that loss of TIM2 causes replisome malfunctioning ultimately leading to DSBs [22, 23]. In a wild-type background, most of these DSBs would be repaired through the dual activity of *mei-41*, leading to a relatively modest increase in the frequency of chromosome aberrations. However, when *mei-41* function is compromised, most DSBs would not be properly repaired because of a combined defect in DNA repair and checkpoint-mediated cell-cycle delay, resulting in extensive chromosome fragmentation.

TIM2 orthologs have been reported to collaborate in maintaining the integrity of the replisome under stress conditions such as hydroxyurea (HU)-induced deoxyribonucleotide triphosphate (dNTP) pool depletion [14]. Thus, we monitored chromosome aberrations in HU-treated wild-type, *PBtim2⁻*, and *mei-41^29D* larval brains. *PBtim2⁻* brains showed a significant increase in chromosome breakage compared to wild-type. Consistent with previous results [24], HU treatment also caused a dramatic increase in chromosome damage in *mei-41^29D* mutant brains (Figures 4H–4K). In these brains, the frequency of metaphases with shattered chromosomes was significantly higher than in HU-treated *PBtim2⁻* brains. This supports the view that *tim2* and *mei-41* do not function in a single linear pathway leading to chromosome aberrations. In keeping with our model (Figure 4N), we propose that TIM2 depletion greatly potentiates the primary DNA damage induced by HU, thereby causing extensive chromosome instability even in the presence of wild-type *mei-41* activity.

We also investigated whether *Drosophila tim2* plays a role in the assembly of non-SMC cohesin subunits, as reported for its *C. elegans* ortholog [13]. In wild-type brain cells, the non-SMC cohesin RAD21 localizes to the mitotic chromosomes and is enriched in the heterochromatic regions. No significant change in RAD21 localization was observed in *PBtim2^c06976* mutants, suggesting that *Drosophila* TIM2 is not required for cohesin-dependent integrity of mitotic chromosomes (Figure S4).
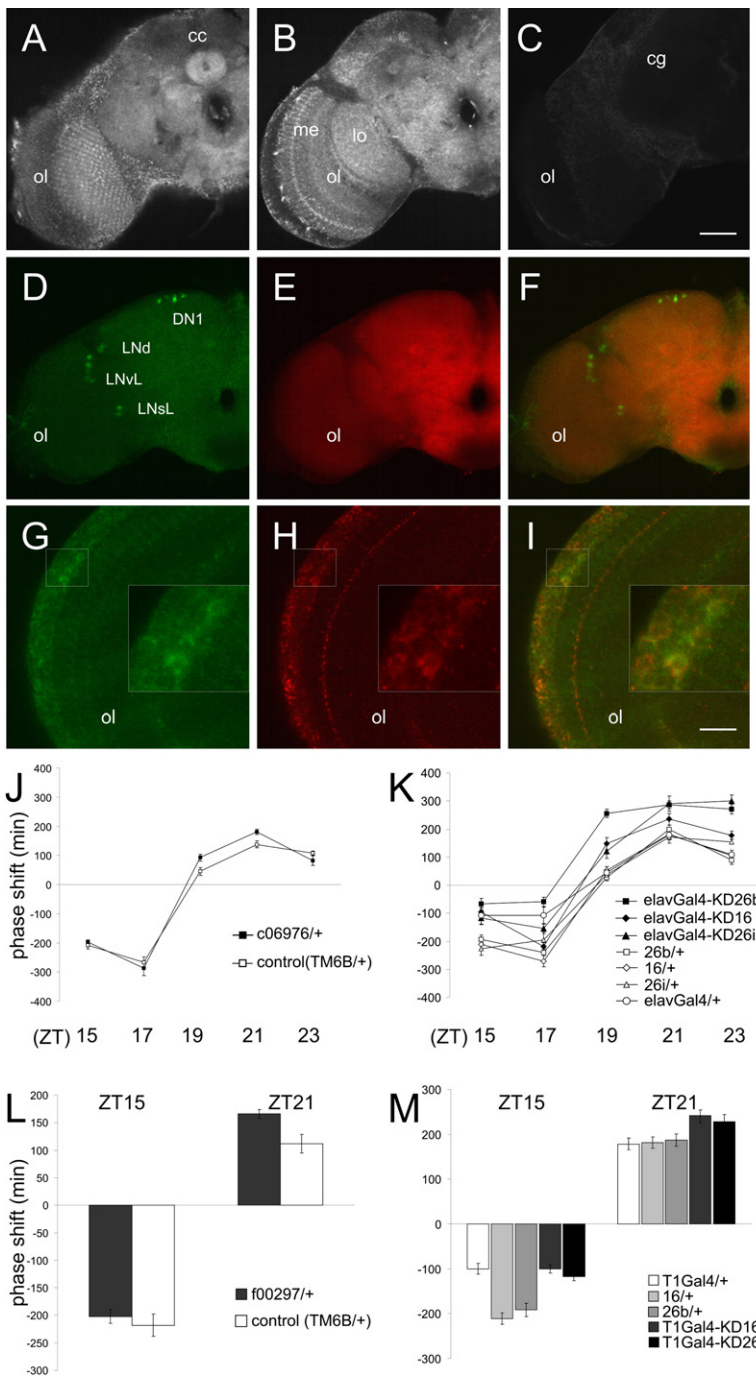
Figure 3. *tim2* in Adult Flies: Expression in Brain and Role in Circadian Light Entrainment

(A–I) mRNA localization in whole-mount adult brains sampled at ZT1. The following abbreviations are used: ol, optic lobe; cc, central complex; me, medulla; lo, lobula; cg, central ganglion; LNvL, large lateral ventral neurons; LNvS, small lateral ventral neurons; LNd, lateral dorsal neurons; DN1, dorsal neuron group 1. Scale bar in (C) represents 50 μm for (A)–(F); scale bar in (I) represents 30 μm for (G)–(I) and 10 μm in the 3× magnification insets in (G)–(I).

(A–C) Wild-type (*w^{1118}*) brains hybridized with an antisense (A and B) or a sense *tim2* mRNA probe (negative control, C). (A) and (B) show confocal sections obtained from the same brain within a 30 μm interval along the anterior-posterior axis.

(D–F) Double-labeling in situ hybridization on wild-type brains of *cry* (green, D) and *tim2* (red, E) mRNAs; signals are merged in (F). Images are ~40 μm Z projections of 18 confocal sections.

(G–I) Localization of β-*gal* (green, G) and *tim2* (red, H) mRNAs in *T1Gal4-UASlacZ* adult brains; signals are merged in (I). β-*gal* and *tim2* mRNAs colocalize in some of the T1 cell bodies.

(J–M) *tim2* downregulation affects circadian phase responses to light. Advances and delays in phase response (mean ± SEM) are represented as positive and negative values, respectively.

(J) Phase-response curve (PRC) for *PBtim2^{c06976}*/+ and *TM6B*/+ (control) flies. The PRC of *PBtim^{c06976}*/+ flies was significantly different from that of *TM6B*/+ controls (genotype × time [ZT] interaction $F_{4,373}$ = 5.56, p = 0.0002; post hoc test for ZT19 and ZT21, p < 0.01 with respect to *TM6B*/+ control).

(K) PRCs for *elavGal4-tim2* KD^{26b}, *elavGal4-tim2* KD^{16}, and *elavGal4-tim2* KD^{26i} lines and relative controls *tim2* KD^{26b}/+, *tim2* KD^{16}/+, *tim2* KD^{26i}/+, and *elavGal4*/+. PRCs of *elavGal4-tim2* KD lines with respect to their corresponding controls: analysis of variance genotype × time (ZT) interactions $F_{24,1260}$ = 5.24, p < 0.00001. Post hoc tests revealed that all *elavGal4-tim2* KD lines were significantly more reactive to light pulses in the advance zone.

(L) *PBtim2^{f00297}*/+ heterozygotes revealed a significant enhancement in phase advances at ZT21 compared to controls (*TM6B*/+; $F_{1,65}$ = 8.17, p < 0.01).

(M) Phase responses for *T1Gal4-tim2* KD^{16} and *T1Gal4-tim2* KD^{26b} were significantly enhanced at ZT21 compared to corresponding controls ($F_{4,143}$ = 5.11, p = 0.0007). At ZT15, *T1Gal4-tim2* KD^{16} and *T1Gal4-tim2* KD^{26b} were not significantly different from their *T1Gal4*/+ controls (see also Table S2).

tim2 Downregulation Does Not Affect Adult Circadian Locomotor Activity in Constant Darkness

Whether the *timeless2* gene family plays a role in the circadian clock has been intensely debated [25–28]. In mammals, homozygous *mTim* mutants die as embryos, whereas viable *mTim$^-$*/+ heterozygotes do not show circadian behavioral abnormalities [2]. However, *mTim* disruption affects phasing of suprachiasmatic nuclei neuronal activity rhythms and clock protein expression [5].

We analyzed the effects of *tim2* inhibition on the free-running periodicity of locomotor activity in DD. An examination of *PBtim2^{c06976}*/+ and *PBtim2^{f00297}*/+ adults did not show significant period length (τ) changes compared to controls

(Table S1). Locomotor rhythmicity was also evaluated in adult flies in which *tim2* was silenced by RNA interference in specific brain regions. With a series of *Gal4* drivers, *tim2* was silenced in the central nervous system (CNS; *elavGal4*), in circadian clock neurons (*tim1Gal4* and *pdfGal4*), in mushroom bodies and optic lobes (*OK107Gal4*) [29], in L1 and L2 lamina monopolar cells and in the central complex (*L1L2Gal4*) [8], in medulla T1 basket cells of the optic lobes (*T1Gal4*) [8], and in the eye R1–R8 photoreceptors (*GMRGal4*). In all *tim2* KD-driver combinations, periods were well within the normal wild-type ranges of 23.7 hr to 24.9 hr, and none of the combinations was significantly different from the corresponding controls (Table S1).

Table 1. Molecular Characterization of *PBtim2⁻* Mutant Alleles

	% of mRNA Levels (Mean ± SEM)			
Genotype	*tim2*	*CG34308*	*BK 002510*	*2mit*
c06976/c06976	12 ± 1.7[a]	46 ± 13[b]	277 ± 84[c]	105 ± 19
c06976/+	64 ± 4	ND	ND	ND
c01927/c01927	8 ± 2.3[a]	11 ± 2[b]	43 ± 13	94 ± 2
f00297/f00297	2.3 ± 0.1[a]	49 ± 11[b]	116 ± 34	104 ± 20
f05903/f05903	15 ± 5[a]	89 ± 4	83 ± 17	74 ± 20
c03963/c03963	100 ± 0.6	ND	ND	47 ± 5.4[d]
w¹¹¹⁸ (control)	100	100	100	100

mRNA levels of *tim2* and expressed host intronic sequences (*CG34308*, *BK002510*, and *2mit*) in *PBtim2⁻* mutant alleles. Statistical analyses were performed by comparing the mRNA levels of mutant larvae (homozygous or heterozygous) with those of *w¹¹¹⁸* control larvae. ND indicates not determined.

[a] *tim2* mRNA level significantly different from controls ($F_{5,15}$ = 34.57, $p < 0.001$). Post hoc tests revealed similar *tim2* mRNA levels in *PBtim2^c06976*, *PBtim2^c01927*, *PBtim2^f00297*, and *PBtim2^f05903* homozygous larvae ($p > 0.05$, not significant, for the four comparisons).
[b] *CG34308* mRNA level significantly different from controls ($F_{4,11}$ = 32.61, $p < 0.0001$).
[c] *BK002510* mRNA level significantly different from controls ($F_{4,8}$ = 7.22, $p < 0.05$).
[d] *2mit* mRNA level significantly different from controls ($F_{5,11}$ = 3.85, $p = 0.03$).

tim2 Is Involved in Circadian Light Entrainment

We recorded locomotor activity under constant bright light (LL) for *PBtim2^c06976*/+ and *PBtim2^f00297*/+ heterozygotes and flies bearing a *tim2* KD construct driven in the CNS or in the eye photoreceptors (with *elavGal4* or *GMRGal4* drivers, respectively; Table S1). All of these mutant animals displayed wild-type behavior, with ~90% of flies becoming arrhythmic after 1 or 2 days of LL and the remainder showing weak and sometimes long period rhythms (Table S1), consistent with previous studies [30].

We next studied the ability of heterozygous *PBtim^c06976*/+ and *elavGal4* KD flies to respond to 20 min light pulses delivered at different times of the night (ZT15, 17, 19, 21, and 23). We initially determined the *ls-tim1/s-tim1* genotype of each strain, because this natural *tim1* polymorphism significantly affects the circadian light response (Table S2) [31–34]. We generated a light-induced phase response curve (PRC) and observed that heterozygous *ls/s-tim1; PBtim^c06976*/+ flies were significantly more reactive than their corresponding *ls/s-tim1; TM6B*/+ controls in the advance zone at ZT19 and ZT21 (Figure 3J).

PRC profiles similar to that of *PBtim2^c06976*/+ flies were obtained when *tim2* KD was driven panneuronally by *elavGal4*, again with a significantly more reactive response to light pulses in the advance, but not in the delay zone (Figure 3K). We also examined the phase shifts to light pulses delivered at ZT15 and ZT21 in *PBtim2^f00297*/+ heterozygotes (Figure 3L; see also Table S2). These flies, like their KD and *PBtim^c06976*/+ counterparts, revealed a significant increase in their phase responses at ZT21 compared to their relative controls, whereas no significant differences were seen at ZT15.

To map eye or brain structures involved in the control of circadian light entrainment, we used KD lines in which *tim2* was silenced with *GMRGal4*, *L1L2Gal4*, *OK107Gal4*, *tim1Gal4*, *pdfGal4*, and *T1Gal4* drivers (Table S2). An enhancement of the phase shift in the advance zone was observed only when *tim2* KD was driven by the *T1Gal4* driver, as in *PBtim2⁻*/+ and *elavGal4*-driven *tim2* KD flies. However, when the light pulses were administered at ZT15, the same flies were not

significantly different from their *T1Gal4*/+ controls (Figure 3M; see also Table S2). *tim2* silencing in all photoreceptors (with the *GMRGal4* driver) did not produce changes in the phase response to light, suggesting that R7 and R8 photoreceptors are not directly involved in the *tim2*-mediated phenotype (Table S2). Negative results were also obtained by driving *tim2* KD in L1 and L2 monopolar cells (Table S2), which receive information from retinal photoreceptors [9, 10]. *tim2* KD in the other brain compartments, such as mushroom bodies (*OK107Gal4* driver) or circadian clock neurons (with the *tim1Gal4* and *pdfGal4* drivers), did not significantly affect phase shift at either ZT15 or ZT21 (Table S2).

T1 neurons contribute to *Drosophila* motion detection in particular environmental conditions [8]. Our results reveal an additional involvement of these neurons in light input perception and/or transmission to the circadian clock. Because T1 cells do not receive direct inputs from photoreceptors [9] and T1 outputs have not been anatomically mapped [10], the pathway from T1 cells to the clock remains obscure. The T1 driver is also expressed in the mushroom bodies [8], but we excluded a role of this region by using the *OK107* driver, which is expressed throughout the mushroom bodies [29]. Thus, our findings demonstrate that T1 neurons are important intermediates in the circadian light input pathway. It is possible that the observed effects on entrainment are a consequence of damage to the basket cells during development induced by *tim2* KD. However, the presence of *tim2* in adult nerve fibers argues for a specific physiological role of TIM2 in light entrainment.

Although *mTim* mRNA levels in mammals are not modified [27] or are modified only weakly [28] by light pulses in the brain master clock, a circadian expression has been described in the retina [26, 27]. It would be interesting to investigate whether these data imply a conserved role in light entrainment for the mammalian TIM2 ortholog. To date, we are unable to determine whether the absence of delay effects is due to a differential sensitivity to *tim2* depletion in T1 neurons or to the existence of other neurons dedicated to the delay component of entrainment. Future work will focus on the circadian role of the T1 basket cells and how they disseminate light information to the circadian clock neurons.

Conclusions

Our results indicate that *Drosophila* *tim2* is a pleiotropic gene that plays an essential role in the maintenance of chromosome integrity and has an additional function in the light entrainment of the circadian clock (see Table S3 for a comparative overview of *tim2* orthologs among worms, flies, and mammals). Because the *tim2*-derived paralog *tim1* is the canonical light-sensitive component of the fly circadian clock, the light entrainment activity of *tim2* would appear to represent a residual function that was considerably enhanced and extended by the evolution of the *tim1* paralog.
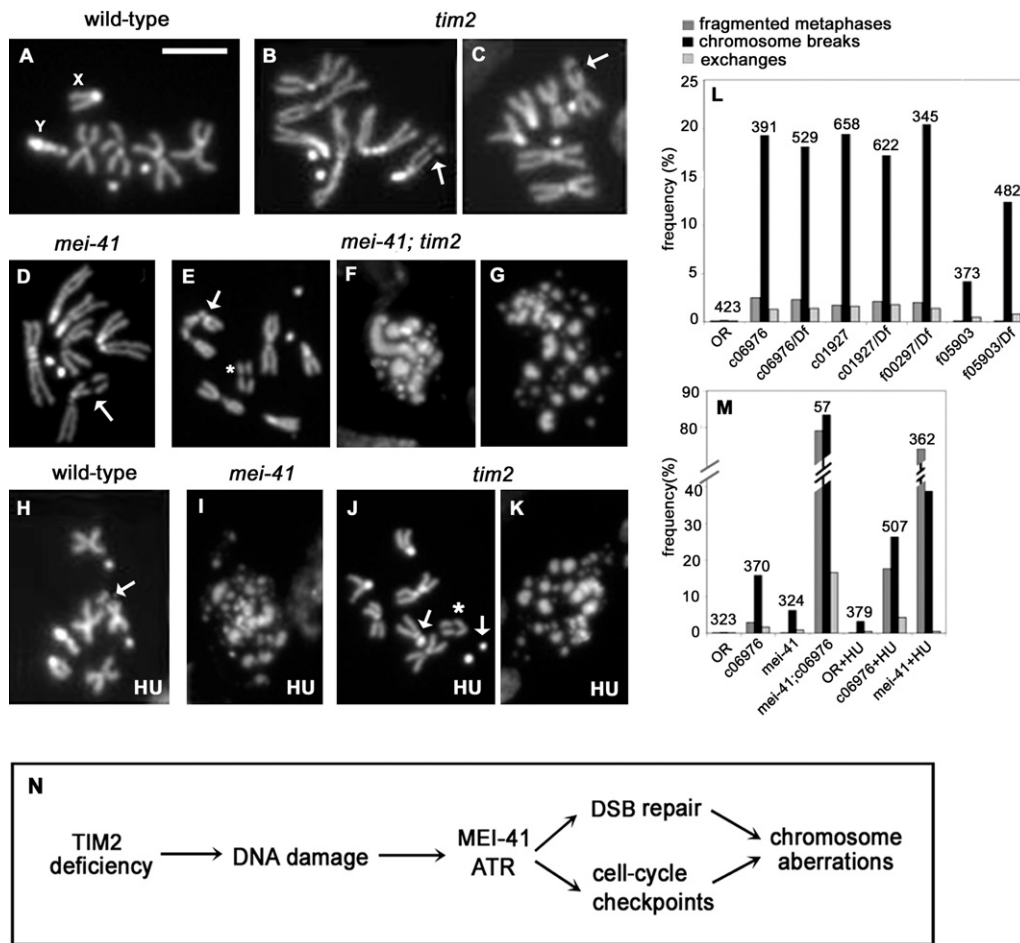
Figure 4. *tim2* Is Required for Chromosome Integrity

(A–K) Metaphase chromosomes from Oregon-R wild-type and mutant larval brains either untreated (A–G) or treated with hydroxyurea (HU) (H–K). Scale bar in (A) represents 5 μm.

(A) Wild-type male metaphase.

(B and C) *tim2* metaphases showing isochromatid breaks (arrows).

(D) *mei-41* metaphase with an isochromatid break (arrow).

(E–G) Metaphase figures from a *mei-41; PBtim2^{c06976}* double mutant showing a dicentric chromosome (arrow) and the corresponding acentric fragment (asterisk) (E) or extensive chromosome fragmentation (F and G).

(H) HU-treated wild-type metaphase with an isochromatid break (arrow).

(I–K) Examples of aberrant metaphase figures observed in HU-treated brains from *mei-41* (I) or *tim2* (J and K) mutants. Mitotic figures in (I) and (K) display multiply fragmented chromosomes; the metaphase in (J) exhibits an incomplete translocation between the third and fourth chromosomes. The centric fragments of chromosomes 3 and 4 are indicated by arrows; the asterisk indicates the acentric fragment of chromosome 3.

(L) Frequencies of cells with chromosome aberrations in *tim2* homozygous and hemizygous mutants. The frequencies observed in *PBtim2^{c06976}/PBtim2^{c06976}*, *PBtim2^{c06976}/Df*, *PBtim2^{c01927}/PBtim2^{c01927}*, *PBtim2^{c01927}/Df*, and *PBtim2^{f00297}/Df* mutants were not significantly different (χ^2 test). *Df* is a deficiency (namely *Df(3R)Exe16177*) that removes the *tim2* locus. OR represents wild-type Oregon-R stock used as control.

(M) Functional relationships between *tim2* and *mei-41* in the maintenance of chromosome integrity. The frequencies of cells with extensive chromosome fragmentation, chromosome breaks, or exchanges observed in HU-treated *PBtim2^{c06976}* homozygotes (*PBtim2^{c06976}* + HU) were significantly lower than those observed in HU-treated *mei-41* mutants (*mei-41* + HU) ($p < 0.001$, $p < 0.01$, and $p < 0.001$, respectively; χ^2 test). OR represents Oregon-R control. In both (L) and (M), the frequencies of cells with chromosome breaks (isochromatid and chromatid deletions) or exchanges (dicentric chromosomes and translocations) were calculated excluding the cells with extensive chromosome fragmentation. The numbers on top of each group of columns correspond to the number of cells scored.

(N) A model for the interaction between *tim2* and *mei-41*. Loss of TIM2 causes replisome malfunctioning, ultimately leading to double-strand breaks (DSBs). Most of these DSBs are repaired through the dual activity of *mei-41*, which delays cell-cycle progression and mediates DNA repair. When *mei-41* is mutated, failure to repair DSBs leads to extensive chromosome fragmentation.

References

1. Benna, C., Scannapieco, P., Piccin, A., Sandrelli, F., Zordan, M., Rosato, E., Kyriacou, C.P., Valle, G., and Costa, R. (2000). A second *timeless* gene in *Drosophila* shares greater sequence similarity with mammalian *tim*. Curr. Biol. *10*, R512–R513.

2. Gotter, A.L., Manganaro, T., Weaver, D.R., Kolakowski, L.F., Jr., Possidente, B., Sriram, S., MacLaughlin, D.T., and Reppert, S.M. (2000). A time-less function for mouse *timeless*. Nat. Neurosci. *3*, 755–756.

3. Rubin, E.B., Shemesh, Y., Cohen, M., Elgavish, S., Robertson, H.M., and Bloch, G. (2006). Molecular and phylogenetic analyses reveal mammalian-like clockwork in the honey bee (*Apis mellifera*) and shed new light on the molecular evolution of the circadian clock. Genome Res. *16*, 1352–1365.

4. Zheng, X., and Sehgal, A. (2008). Probing the relative importance of molecular oscillations in the circadian clock. Genetics *178*, 1147–1155.

5. Barnes, J.W., Tischkau, S.A., Barnes, J.A., Mitchell, J.W., Burgoon, P.W., Hickok, J.R., and Gillette, M.U. (2003). Requirement of mammalian *Timeless* for circadian rhythmicity. Science *302*, 439–442.

6. Cavener, D.R., and Ray, S.C. (1991). Eukaryotic start and stop translation sites. Nucleic Acids Res. *19*, 3185–3192.

7. Claridge-Chang, A., Wijnen, H., Naef, F., Boothroyd, C., Rajewsky, N., and Young, M.W. (2001). Circadian regulation of gene expression systems in the *Drosophila* head. Neuron *32*, 657–671.

8. Rister, J., Pauls, D., Schnell, B., Ting, C.Y., Lee, C.H., Sinakevitch, I., Morante, J., Strausfeld, N.J., Ito, K., and Heisenberg, M. (2007). Dissection of the peripheral motion channel in the visual system of *Drosophila melanogaster*. Neuron *56*, 155–170.

9. Meinertzhagen, I.A., and O'Neil, S.D. (1991). Synaptic organization of columnar elements in the lamina of the wild type in *Drosophila melanogaster*. J. Comp. Neurol. *305*, 232–263.

10. Takemura, S.Y., Lu, Z., and Meinertzhagen, I.A. (2008). Synaptic circuits of the *Drosophila* optic lobe: the input terminals to the medulla. J. Comp. Neurol. *509*, 493–513.

11. Kiebler, M.A., and Bassell, G.J. (2006). Neuronal RNA granules: Movers and makers. Neuron *51*, 685–690.

12. Richter, J.D., and Klann, E. (2009). Making synaptic plasticity and memory last: Mechanisms of translational regulation. Genes Dev. *23*, 1–11.

13. Chan, R.C., Chan, A., Jeon, M., Wu, T.F., Pasqualone, D., Rougvie, A.E., and Meyer, B.J. (2003). Chromosome cohesion is regulated by a clock gene paralogue TIM-1. Nature *423*, 1002–1009.

14. Gotter, A.L., Suppa, C., and Emanuel, B.S. (2007). Mammalian TIMELESS and Tipin are evolutionarily conserved replication fork-associated factors. J. Mol. Biol. *366*, 36–52.

15. Kondratov, R.V., and Antoch, M.P. (2007). Circadian proteins in the regulation of cell cycle and genotoxic stress responses. Trends Cell Biol. *17*, 311–317.

16. Unsal-Kaçmaz, K., Mullen, T.E., Kaufmann, W.K., and Sancar, A. (2005). Coupling of human circadian and cell cycles by the timeless protein. Mol. Cell. Biol. *25*, 3109–3116.

17. Cimprich, K.A., and Cortez, D. (2008). ATR: An essential regulator of genome integrity. Nat. Rev. Mol. Cell Biol. *9*, 616–627.

18. Urtishak, K.A., Smith, K.D., Chanoux, R.A., Greenberg, R.A., Johnson, F.B., and Brown, E.J. (2009). Timeless maintains genomic stability and suppresses sister chromatid exchange during unperturbed DNA replication. J. Biol. Chem. *284*, 8777–8785.

19. Laurençon, A., Purdy, A., Sekelsky, J., Hawley, R.S., and Su, T.T. (2003). Phenotypic analysis of separation-of-function alleles of MEI-41, Drosophila ATM/ATR. Genetics *164*, 589–601.

20. Oikemus, S.R., Queiroz-Machado, J., Lai, K., McGinnis, N., Sunkel, C., and Brodsky, M.H. (2006). Epigenetic telomere protection by *Drosophila* DNA damage response pathways. PLoS Genet. *2*, e71.

21. LaRocque, J.R., Jaklevic, B., Su, T.T., and Sekelsky, J. (2007). *Drosophila* ATR in double-strand break repair. Genetics *175*, 1023–1033.

22. Heller, R.C., and Marians, K.J. (2006). Replisome assembly and the direct restart of stalled replication forks. Nat. Rev. Mol. Cell Biol. *7*, 932–943.

23. Tourrière, H., and Pasero, P. (2007). Maintenance of fork integrity at damaged DNA and natural pause sites. DNA Repair (Amst.) *6*, 900–913.

24. Banga, S.S., Shenkar, R., and Boyd, J.B. (1986). Hypersensitivity of *Drosophila mei-41* mutants to hydroxyurea is associated with reduced mitotic chromosome stability. Mutat. Res. *163*, 157–165.

25. Zylka, M.J., Shearman, L.P., Levine, J.D., Jin, X.W., Weaver, D.R., and Reppert, S.M. (1998). Molecular analysis of mammalian timeless. Neuron *21*, 1115–1122.

26. Sangoram, A.M., Saez, L., Antoch, M.P., Gekakis, N., Staknis, D., Whiteley, A., Fruechte, E.M., Vitaterna, M.H., Shimomura, K., King, D.P., et al. (1998). Mammalian circadian autoregulatory loop: A *timeless* ortholog and m*Per1* interact and negatively regulate CLOCK-BMAL1-induced transcription. Neuron *21*, 1101–1113.

27. Takumi, T., Nagamine, Y., Miyake, S., Matsubara, C., Taguchi, K., Takekida, S., Sakakida, Y., Nishikawa, K., Kishimoto, T., Niwa, S., et al. (1999). A mammalian ortholog of *Drosophila timeless*, highly expressed in SCN and retina, forms a complex with mPER1. Genes Cells *4*, 67–75.

28. Tischkau, S.A., Barnes, J.A., Lin, F.J., Myers, E.M., Barnes, J.W., Meyer-Bernstein, E.L., Hurst, W.J., Burgoon, P.W., Chen, D., Sehgal, A., and Gillette, M.U. (1999). Oscillation and light induction of timeless mRNA in the mammalian circadian clock. J. Neurosci. *19*, RC15.

29. Aso, Y., Grübel, K., Busch, S., Friedrich, A.B., Siwanowicz, I., and Tanimoto, H. (2009). The mushroom body of adult *Drosophila* characterized by GAL4 drivers. J. Neurogenet. *23*, 156–172.

30. Dissel, S., Codd, V., Fedic, R., Garner, K.J., Costa, R., Kyriacou, C.P., and Rosato, E. (2004). A constitutively active *cryptochrome* in *Drosophila melanogaster*. Nat. Neurosci. *7*, 834–840.

31. Peschel, N., Veleri, S., and Stanewsky, R. (2006). *Veela* defines a molecular link between Cryptochrome and Timeless in the light-input pathway to *Drosophila*'s circadian clock. Proc. Natl. Acad. Sci. USA *103*, 17313–17318.

32. Tauber, E., Zordan, M., Sandrelli, F., Pegoraro, M., Osterwalder, N., Breda, C., Daga, A., Selmin, A., Monger, K., Benna, C., et al. (2007). Natural selection favors a newly derived *timeless* allele in *Drosophila melanogaster*. Science *316*, 1895–1898.

33. Sandrelli, F., Tauber, E., Pegoraro, M., Mazzotta, G., Cisotto, P., Landskron, J., Stanewsky, R., Piccin, A., Rosato, E., Zordan, M., et al. (2007). A molecular basis for natural selection at the timeless locus in *Drosophila melanogaster*. Science *316*, 1898–1900.

34. Peschel, N., Chen, K.F., Szabo, G., and Stanewsky, R. (2009). Light-dependent interactions between the *Drosophila* circadian clock factors cryptochrome, jetlag, and timeless. Curr. Biol. *19*, 241–247.